



This open access document is posted as a preprint in the Beilstein Archives at <https://doi.org/10.3762/bxiv.2020.112.v1> and is considered to be an early communication for feedback before peer review. Before citing this document, please check if a final, peer-reviewed version has been published.

This document is not formatted, has not undergone copyediting or typesetting, and may contain errors, unsubstantiated scientific claims or preliminary data.

Preprint Title Circularly Polarized Luminescent Systems Fabricated by Tröger's Base Derivatives through Two Different Strategies

Authors Cheng Qian, Yuan Chen, Qian Zhao, Ming Cheng, Chen Lin, Juli Jiang and Leyong Wang

Publication Date 01 Oct 2020

Article Type Letter

Supporting Information File 1 002 BJOC-SI-qiancheng-2020-10-01.pdf; 872.7 KB

ORCID® IDs Juli Jiang - <https://orcid.org/0000-0001-5778-6380>; Leyong Wang - <https://orcid.org/0000-0001-5775-3714>

Circularly Polarized Luminescent Systems Fabricated by Tröger's Base Derivatives through Two Different Strategies

Cheng Qian^{‡,1}, Yuan Chen^{‡,1}, Qian Zhao¹, Ming Cheng¹, Chen Lin¹, Juli Jiang^{*1}, and Leyong Wang^{*1,2}

Address:

¹Key Laboratory of Mesoscopic Chemistry of MOE, Jiangsu Key Laboratory of Advanced Organic Materials, School of Chemistry and Chemical Engineering, Nanjing University, Nanjing, 210023, China

²Advanced Materials Institute, Qilu University of Technology (Shandong Academy of Sciences), Jinan, 250014, China

E-mail:

jji@nju.edu.cn, lywang@nju.edu.cn

*Corresponding authors

‡Equal contributors

Abstract

Tröger's base derivative **rac-TBPP** was synthesized and separated into two enantiomers **R_{2N}-TBPP** and **S_{2N}-TBPP** by chiral column, which emit strong circularly polarized luminescence with g_{lum} values of +0.0021, and -0.0025, respectively. The different way to fabricate the CPL-active material is to cogel the fluorescent **rac-TBPP** with a chiral *D*-glutamic acid gelator **DGG** by co-assembly strategies. At the molar ratio of **rac-TBPP** : **DGG** = 1 : 80, the g_{lum} value of the cogel was increased to be about

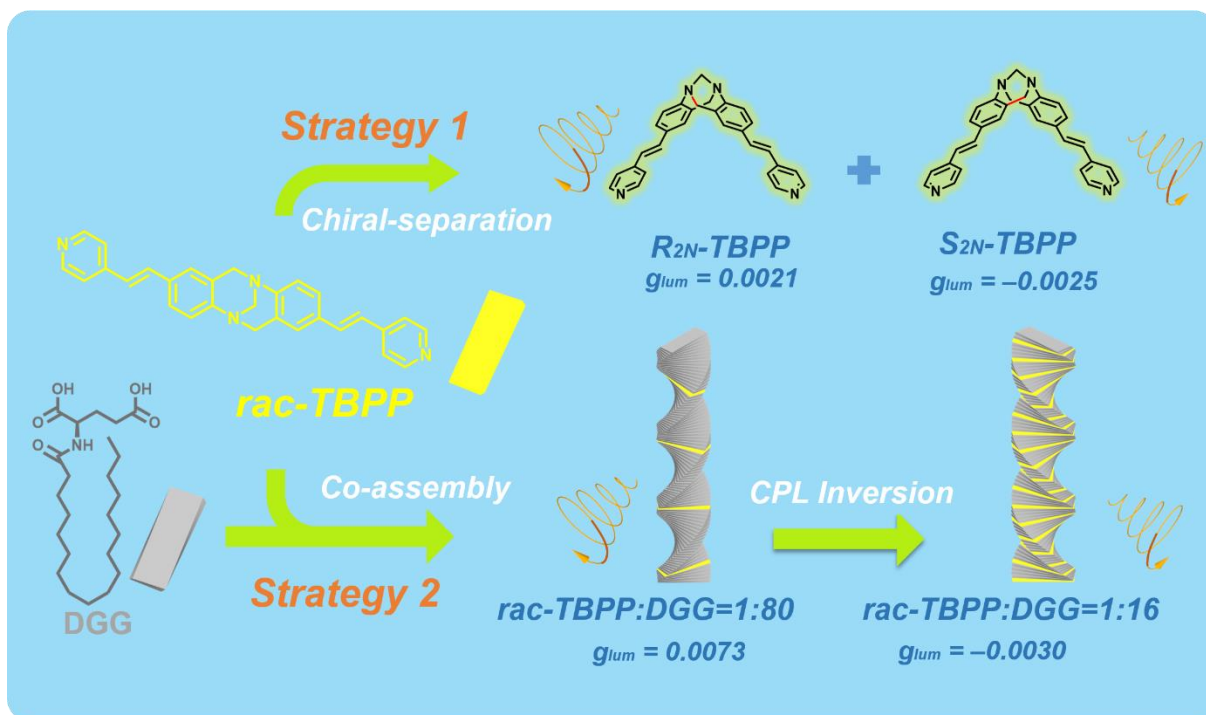
three times higher than that observed from ***R*_{2N}-TBPP** and ***S*_{2N}-TBPP** enantiomers. Interestingly, the CPL handedness of the ***rac*-TBPP/DGG** cogel could be adjusted effectively by changing their stoichiometric ratios.

Keywords

Tröger's base; circularly polarized luminescence; chiral resolution; co-gelation; inversion of CPL handedness

Introduction

Recently, much effort has been devoted to constructing the luminescent materials with efficient high emission in the solid state [1-3]. More and more types of fluorophores with aggregation-induced emission (AIE) characteristics have been discovered and applied in practice [4-6]. Among them, the fluorescent materials emitting circular polarized luminescence (CPL) have attracted intensive interest owing to their wide applications in various researching field including 3D displays, chiroptical materials, and so on [7-10]. Circular dichroism (CD) absorption spectrum reflects the chirality of the fluorescent materials in the ground state, and circularly polarized luminescence (CPL) spectrum reflects the chirality of fluorescent materials in the excited electronic state. So CD spectrum and CPL spectrum are two most important tools to test the chirality of luminescent materials [11-12].



Scheme 1. Cartoon representative for CPL systems fabricated by **TBPP** through two different strategies

As a useful building block in constructing functional material [13-14], Tröger's base (TB), first synthesized in 1887 [15], shows high controllability and obvious advantages. Without considering the side chain there are eleven sites in its framework that could be modified, and the loose stacking of TB unit could reduce the distance-dependent intermolecular quenching effect in the aggregation state, which caused by its V-configuration [16]. Moreover, large dihedral angle of TB (80-104°) [15] permits less self-absorption and wider stokes shift [17]. Further, steric hindrance and highly rigidity could reduce non-radioactive transition and restrict the internal rotation [18]. Although TB shows excellent performance in constructing AIE materials, its derivatives emitting CPL have rarely been reported. To construct a CPL-active material, a luminescent part and a chiral part are necessary [19-21]. As far as TB is concerned, it can be modified

to be a luminescent material building block, and its bridged methylene groups of diazocine chiral nitrogen atoms prevent the inversion of the configuration, and two enantiomers could be formed then. Herein, we take two strategies to construct Tröger's base derivatives **TBPP**-based CPL material. One method is to separate non-CPL emission *rac*-**TBPP** into CPL-active enantiomers **R_{2N}-TBPP** and **S_{2N}-TBPP**. The other strategy is to co-assemble the fluorescent *rac*-**TBPP** with a chiral *D*-glutamic acid gelator **DGG** to form the CPL-active cogel. Interestingly, adjusting the stoichiometric ratios of *rac*-**TBPP**/**DGG** of the co-assembling system, the handedness of CPL-active cogel can be controlled effectively.

Results and Discussion

The synthetic routes of *rac*-**TBPP** are outlined in Scheme S1. Firstly, 2,8-dibromo-6H,12H-5,11-methanodibenzo[b,f][1,5]diazocine was synthesized according to the reported procedure [22], and then, by Suzuki coupling reaction between 2,8-dibromo-6H,12H-5,11-methanodibenzo[b,f][1,5]diazocine and 4-vinyl pyridine, *rac*-**TBPP** was successfully obtained in 51.8% yield. Detailed experiments and characterization were described in the ESI (Figure S1-S3). Then, *rac*-**TBPP** was separated into two fractions **R_{2N}-TBPP** and **S_{2N}-TBPP** by chiralpak IB column using MeOH/DCM (80/20, v/v) as the eluent (Figure S5). CD spectrum of the first fraction exhibited a positive Cotton effect at 352 nm, assigned to **R_{2N}-TBPP**, while the second one showed a negative Cotton effect at the same wavelength, assigned to **S_{2N}-TBPP** (Figure 1a) [23]. Then, **R_{2N}-TBPP** and **S_{2N}-TBPP** were tested in CPL spectroscopy, and the magnitude of CPL

emission was estimated by a luminescence dissymmetry factor (g_{lum}), defined as $2(I_L - I_R)/(I_L + I_R)$ where I_L and I_R are the intensity of the left-handed and right-handed CPL signals [24], respectively. Ranging from +2 for an ideal left-handed CPL to -2 for an ideal right-handed CPL, g_{lum} value comes up to zero when no circular polarization of the luminescence was detected. The calculated value of g_{lum} of CPL signals for ***R*_{2N}-TBPP** and ***S*_{2N}-TBPP** are +0.0021, and -0.0025, respectively (Figure 1b), which is much larger than many small organic molecules [25].

In order to avoid tedious chiral separation, we try to construct the CPL-active material by co-assembling the achiral fluorophore ***rac*-TBPP** with a chiral gelator. In co-assembly CPL-active systems, achiral fluorophores are always involved in forming the chiral supramolecular structure through non-covalent weak interactions. So, the CPL emission of co-assembly systems could be easy to be adjusted by external stimuli. *D*-glutamic acid gelator **DGG** and its enantiomer **LGG** possess three hydrogen-bond sites, two carboxylic acid groups and one amide, which could form the stable spiral structure

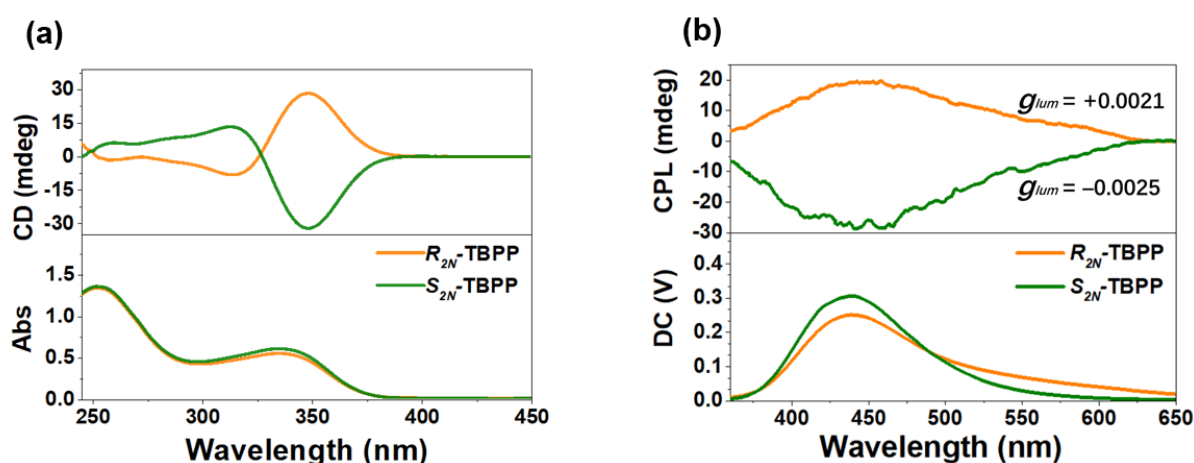


Figure 1. Ground-state and excited-state chirality of R_{2N} -TBPP and S_{2N} -TBPP. (a) CD spectra of R_{2N} -TBPP and S_{2N} -TBPP. (b) CPL spectra of R_{2N} -TBPP and S_{2N} -TBPP excited at 350 nm.

by hydrogen-bond and other non-covalent interactions. **DGG** was synthesised by introducing octadecyl into the glutamic skeleton in 78.6% yield according to the reported route (Scheme S2) [26]. When *rac*-TBPP was mixed with **DGG** at molar ratios from 1/100 to 1/16 (*rac*-TBPP/DGG), transparent yellow cogels were successfully formed by being heated to dissolve in chloroform, and then cooled to ambient temperature (Figure S6). Owing to AIE effect of TB unit the fluorescence intensity of

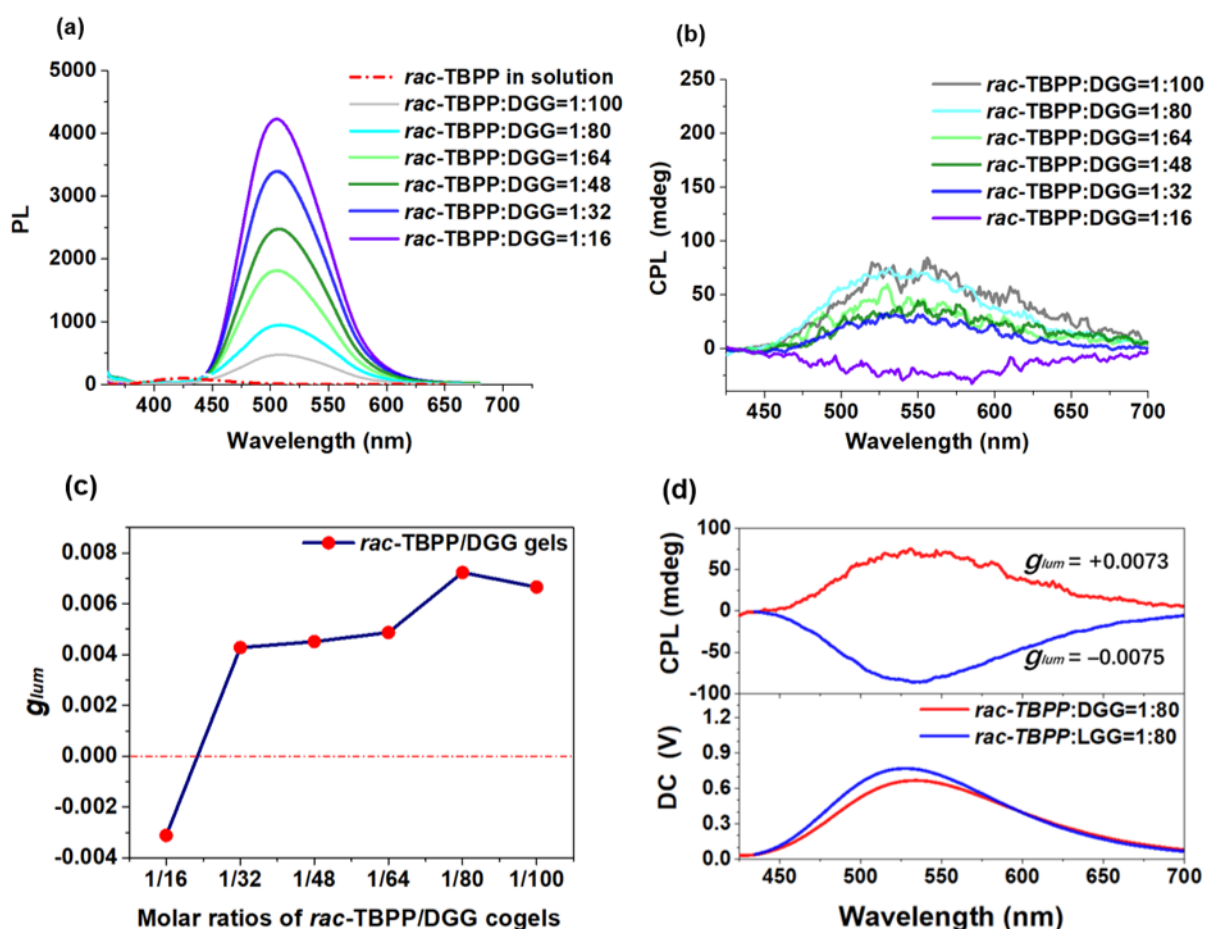


Figure 2. (a) Fluorescence spectra of **rac-TBPP** in solution (dash line) and in the **rac-TBPP/DGG** cogels. (b) CPL spectra of the **rac-TBPP/DGG** cogel at molar ratios from 1:100 to 1:16. (c) Plot of g_{lum} value of CPL signals versus ratios of **rac-TBPP/DGG** in the cogel. (d) Mirror CPL spectra of **rac-TBPP/DGG** and **rac-TBPP/LGG** cogel at the molar ratio of 1:80.

these co-assembly cogels enhanced sharply. At the molar ratio of **rac-TBPP/DGG** = 1 : 16, the CPL spectra of the cogel shows negative Cotton signal. At the molar ratio of **rac-TBPP/DGG** = 1:32 or higher, positive Cotton signal exhibiting left-handed CPL signals were observed (Figure 2b). At the molar ratio of **rac-TBPP/DGG** = 1/80, the CPL spectra shows positive Cotton signal with g_{lum} value about +0.0073, which was almost three times higher than g_{lum} value of **TBPP** enantiomers (Figure 2c).The

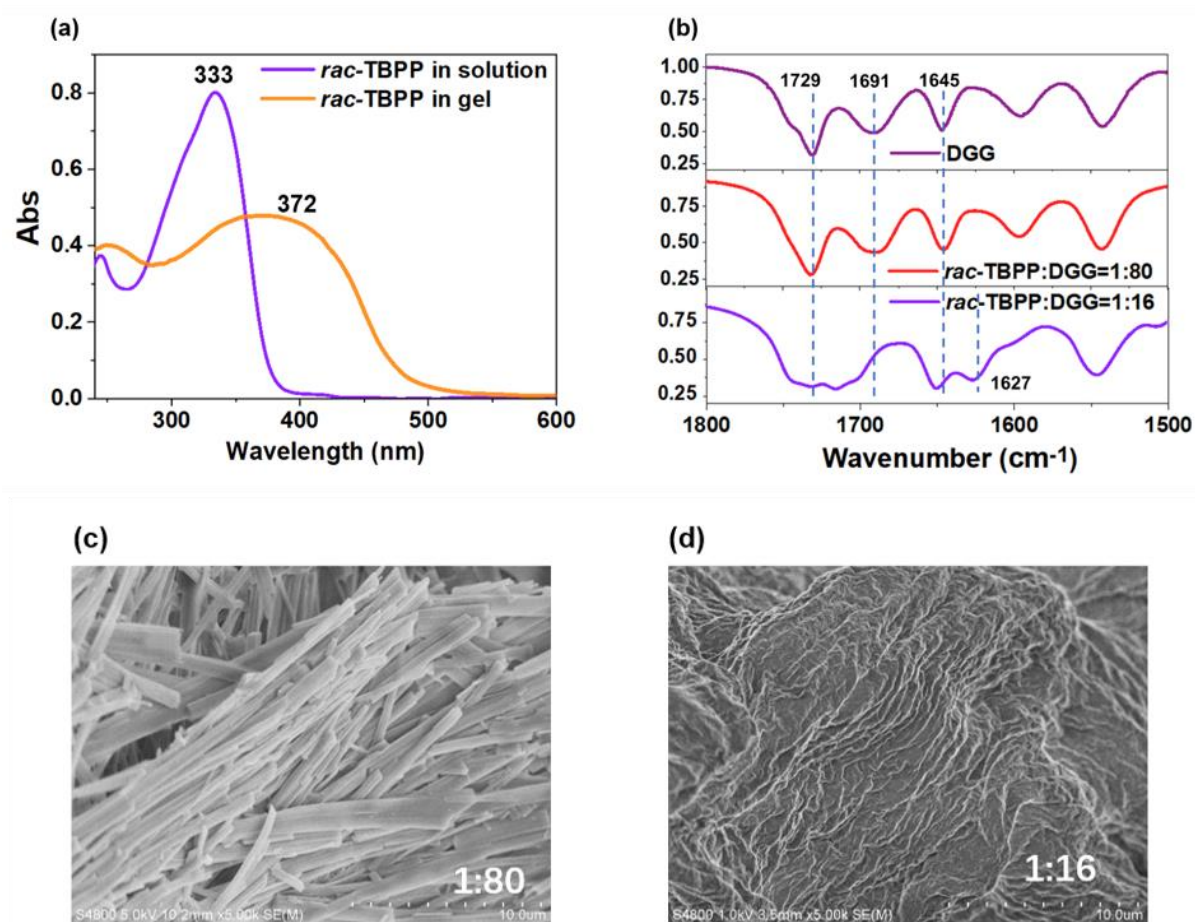


Figure 3. (a) UV-vis absorption spectra of *rac*-TBPP and *rac*-TBPP/DGG cogel (*rac*-TBPP/DGG = 1:80). (b) FT-IR spectra of DGG and *rac*-TBPP/DGG cogels at molar ratios of 1:80 and 1:16, respectively. SEM images of *rac*-TBPP/DGG cogels at molar ratios of 1:80 (c) and 1:16 (d).

chiroptical activity measured from CPL spectra shows an inversion of CPL handedness at the molar ratio of *rac*-TBPP/DGG = 1:16. Mirror patterns were obviously observed in the CPL spectra for DGG and its *L*-enantiomers LGG (Figure 2d).

In order to get an indepth understanding on the inversion of CPL handedness, the *rac*-TBPP/DGG cogels at molar ratios of 1:16 and 1:80 was explored further by UV-vis and FT-IR (fourier transform infrared) spectra. UV-vis absorption spectra of *rac*-TBPP/DGG

cogels exhibits a strong absorption band at 333 nm, assigned to the conjugated structure of benzene and pyridine in the **rac-TBPP** (Figure 3a). However, a red-shift broaden absorption band situated at 372 nm appears in the **rac-TBPP/DGG** cogel, implying the formation of the ordered packing of **rac-TBPP** in supramolecular assemblies. At the molar ratio of **rac-TBPP/DGG** = 1 :80, FT-IR spectra was similar to that of the **DGG** gel, in which $\nu_{C=O}$ bonds at 1729, 1691, and 1645 cm^{-1} reveal that carboxyl acid groups of **DGG** could be involved in the formation of various hydrogen bonds (Figure 3b, Figure S7). At the molar ratio of **rac-TBPP/DGG** = 1 :16, the intensity of the peak at 1691 cm^{-1} decreases, and the peak at 1729 cm^{-1} broadens. A new peak adjacent to 1645 cm^{-1} appears at 1627 cm^{-1} . All results demonstrates that some of the acid–acid hydrogen bonds between **DGG** molecules might be replaced by acid–pyridine hydrogen bonds between **DDG** and **rac-TBPP** [27]. In addition, the influence of the stoichiometric ratios to the morphologies of **rac-TBPP/DGG** cogels was investigated using a scanning electron microscope (SEM). At the molar ratio of **rac-TBPP/DGG** = 1 :80, the cogel shows belt-like nanofibers (Figure 3c) while fibrous morphology could not be observed at the molar ratio of 1:16 (Figure 3d). It indicates that two different kinds of supramolecular assemblies was formed at the ratios of **rac-TBPP/DGG** 1:80 and 1:16, respectively, which is coincident with the inversion of the CPL responses.

Conclusion

In conclusion, two strategies were demonstrated to obtain CPL-active material based

on Tröger's base derivatives **rac-TBPP**. One method is to separate **rac-TBPP** into two enantiomers **R_{2N}-TBPP** and **S_{2N}-TBPP**, which emit strong circularly polarized luminescence. the other strategy is to cogel the fluorescent **rac-TBPP** with a chiral *D*-glutamic acid gelator **DGG** by the co-assembly strategy. The cogels show significant CPL emission and stoichiometry-controlled inversion of chirality due to the hydrogen bonding interactions and packing modes in the supramolecular co-assemblies.

Acknowledgements

We thank Prof. Carsten Schmuck for valuable suggestions and discussion to our researchs on molecular recognition during his visit in Nanjing Univ. in 2011 and afterwards.

Funding

This work was supported by the National Natural Science Foundation of China (Nos. 21901113, 21871135, 21871136), and the Natural Science Foundation of Jiangsu Province (No. BK20190287).

ORCID[®] iDs

Juli Jiang – <https://orcid.org/0000-0001-5778-6380>

Leyong Wang – <https://orcid.org/0000-0001-5775-3714>

References

1. Zhang, Z. Y.; Chen, Y.; Liu, Y. *Angew. Chem. Int. Ed.* **2019**, *58*, 6028-6032. doi:

10.1002/anie.201901882

2. Chen, C.; Chi, Z.; Chong, K. C.; Batsanov, A. S.; Yang, Z.; Mao, Z.; Yang, Z.; Liu, B. *Nat. Mater.* doi: 10.1038/s41563-020-0797-2

3. Bolton, O.; Lee, K.; Kim, H. J.; Lin, K. Y.; Kim, J. *Nat. Chem.* **2011**, *3*, 205-210. doi: 10.1038/NCHEM.984

4. Zhao, Z.; Zhang, H.; Lam, J. W. Y.; Tang, B. Z. *Angew. Chem. Int. Ed.* **2020**, *59*, 9888-9907. doi:10.1002/anie.201916729

5. Li, J.; Wang, J.; Li, H.; Song, N.; Wang, D.; Tang, B. Z. *Chem. Soc. Rev.* **2020**, *49*, 1144-1172. doi:10.1039/C9CS00495E

6. Roose, J.; Tang, B. Z.; Wong, K. S. *Small* **2016**, *12*, 6495-6512. doi:10.1002/smll.201601455

7. Han, J.; Guo, S.; Lu, H.; Liu, S.; Zhao, Q.; Huang, W. *Adv. Optical Mater.* **2018**, *6*, 1800538. doi: 10.1002/adom.201800538

8. Zheng, H.; Li, W.; Li, W.; Wang, X.; Tang, Z.; Zhang, S. X.-A.; Xu, Y. *Adv. Mater.* **2018**, *30*, 1705948. doi: 10.1002/adma.201705948

9. Nitti, A.; Pasini, D. *Adv. Mater.* **2020**, 1908021. doi: 10.1002/adma.201908021

10. Han, J.; You, J.; Li, X.; Duan, P.; Liu, M. *Adv. Mater.* **2017**, *29*, 1606503. doi: 10.1002/adma.201606503

11. Berova, N.; Bari, L. D.; Pescitelli, G. *Chem. Soc. Rev.* **2007**, *36*, 914-931. doi:10.1039/b515476f

12. Sanchez-Carnerero, E. M.; Agarrabeitia, A. R.; Moreno, F.; Maroto, B. L.; Muller, G.; Ortiz, M. J.; de la Moya, S. *Chem. Eur. J.* **2015**, *21*, 13488-13500.

doi:10.1002/chem.201501178

13. Rúnarsson, Ö. V.; Artacho, J.; Wärnmark, K. *Eur. J. Org. Chem.* **2012**, 7015-7041.

doi:10.1002/ejoc.201201249

14. Dolenský, B.; Havlík, M.; Král, V. *Chem. Soc. Rev.* **2012**, *41*, 3839-3858.

doi:10.1039/c2cs15307f

15. Tröger, J. *J. Prakt. Chem.* **1887**, *36*, 225-245. doi:10.1002/prac.18870360123.

16. Yuan, C.-X.; Tao, X.-T.; Ren, Y.; Li, Y.; Yang, J.-X.; Yu, W.-T.; Wang, L.; Jiang, M.-H. *J. Phys. Chem. C* **2007**, *111*, 12811-12816. doi:10.1021/jp0711601

17. Xi, H.; Liu, Y.; Yuan, C.-X.; Li, Y.-X.; Wang, L.; Tao, X.-T.; Ma, X.-H.; Zhang, C.-F.; Hao, Y. *RSC Adv.* **2015**, *5*, 45668-45678. doi:10.1039/c5ra07912h

18. Yuan, R.; Li, M.-q.; Xu, J.-b.; Huang, S.-y.; Zhou, S.-l.; Zhang, P.; Liu, J.-j.; Wu, H. *Tetrahedron* **2016**, *72*, 4081-4084. doi:10.1016/j.tet.2016.05.042

19. Sang, Y.; Han, J.; Zhao, T.; Duan, P.; Liu, M. *Adv. Mater.* **2019**, 1900110.

doi:10.1002/adma.201900110

20. Takaishi, K.; Iwachido, K.; Takehana, R.; Uchiyama, M.; Ema, T. *J. Am. Chem. Soc.* **2019**, *141*, 6185-6190. doi: 10.1021/jacs.9b02582

21. Liang, J.; Guo, P.; Qin, X.; Gao, X.; Ma, K.; Zhu, X.; Jin, X.; Xu, W.; Jiang, L.; Duan, P. *ACS Nano* **2020**, *14*, 3190-3198. doi:10.1021/acsnano.9b08408

22. Yuan, C.; Zhang, Y.; Xi, H.; Tao, X. *RSC Adv.* **2017**, *7*, 55577-55581. doi:10.1039/c7ra11228a

23. Chen, Y.; Cheng, M.; Hong, B.; Zhao, Q.; Qian, C.; Jiang, J.; Li, S.; Lin, C.; Wang, L. *Front. Chem.* **2019**, *7*, 383. doi:10.3389/fchem.2019.00383

24. Riehl, J. P.; Richardson, F. S. *Chem. Rev.* **1986**, *86*, 1-16.
doi:10.1021/cr00071a001
25. Ma, J.-L.; Peng, Q.; Zhao, C.-H.; *Chem. Eur. J.* **2019**, *25*, 15441-15454.
doi:10.1002/chem.201903252
26. Bachl, J.; Mayr, J.; Sayago, F. J.; Cativiela, C.; Díaz Díaz, D. *Chem. Commun.* **2015**, *51*, 5294-5297. doi:10.1039/C4CC08593K
27. Li, P.; Lue, B.; Han, D.; Duan, P.; Liu, M.; Yin, M. *Chem. Commun.* **2019**, *55*, 2194-2197. doi:10.1039/c8cc08924h